Terpenoids: Shape and non-covalent interactions. The rotational spectrum of: Cis -verbenol and its 1 : 1 water complex

Terpenoids: shape and non-covalent interactions. The rotational spectrum of *cis*-verbenol and its 1 : 1 water complex†

Susana Blanco, [a] Juan Carlos López [a] and Assimo Maris *[b]

DOI: 10.1039/d0cp00086h

Verbenols are aromatic terpenoids whose bioactivity is attracting considerable experimental efforts. Exploiting the chirped-pulse Fourier transform technique, the rotational spectra of *cis*-verbenol, its hydroxyl deuterated form, and all ^{13}C-monosubstituted isotopologues have been assigned, allowing for the structure determination, as the knowledge of its shape is crucial to understanding its molecular activity. Unlike in the solid state, in the gas phase, the most stable conformer exhibits an *anti* HO–CH arrangement, analogous to that of simpler allyl alcohol compounds. Observation of the 1 : 1 water complex showed that the conformation of *cis*-verbenol is still *anti* where water not only acts mainly as a proton donor to the hydroxyl group, but also as a proton acceptor, forming a secondary C–H···O interaction with the hydrogen atom of alkyl verbenol.

1 Introduction

Terpenes are a class of cyclic and acyclic organic compounds resulting from the condensation of two or more 2-methyl-1,3-butadiene (isoprene) units. Modified terpenes, including oxidation products, such as epoxides, alcohols, aldehydes, and ketones, are called terpenoids. Meroterpenoids are chemical compounds having a partial terpenoid structure. Overall, the class of isoprene derivatives includes a large number of naturally produced molecules.

Large terpenoids have important biological activities, such as sterols (membrane components and hormones) and carotenoids (photosynthetic pigments and antioxidants). Smaller terpenoids, derived from two or three condensed isoprene units (called mono- and sesquiterpenoids, respectively), are volatile compounds found in plant essential oils. They are also a component of semiochemicals, which are mixtures of molecules secreted or excreted by living organisms for the purpose of communication.

However, new natural roles remain to be discovered for terpenoids, given that a small percentage of them have been investigated so far. Well documented examples of this are pheromones produced by insects to signal members of the same species regarding the presence of mates, food and enemies.[1] It is well known that this kind of communication requires a precise and concrete structure and conformation to give the exact message.

Here, we focus on the behavior of verbenols, a group of bicyclic monoterpenes – alcohols derived from α-pinene. The four known stereoisomers of verbenol are shown in Fig. 1. They are *cis* or *trans*, depending on the relative position of the C9 and C10 methyl groups with respect to the hydroxyl group. Owing to the presence of three stereogenic carbon atoms (C1, C2 and C5), for each form, there are two enantiomers, (+) and (−), respectively. The (±)-*trans* isomers are oils and are diastereoisomers of the (±)-*cis* enantiomeric structures that are solid (m.p. 335–338 K). Verbenols are found in verbena, hyssop, turpentine and incense, and, having a pleasant odour, they are exploited as flavouring ingredients. Myrcene (7-methyl-3-methylene-1,6-octadiene), ipsdienol ((4*S*)-2-methyl-6-methylideneocta-2,7-dien-4-ol) and verbenone are aggregation pheromones of Bark beetles.[2,3]

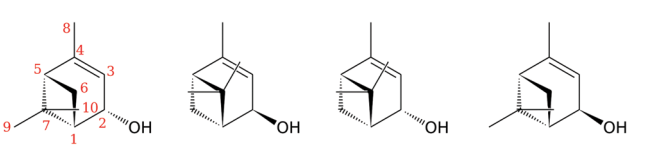

(+)-*cis*-verbenol 1S, 2S, 5S | (-)-*cis*-verbenol 1R, 2R, 5R | (+)-*trans*-verbenol 1R, 2S, 5R | (-)-*trans*-verbenol 1S, 2R, 5S

Fig. 1 Sketch of the four stereoisomers of verbenol and numbering scheme.

[a] *Departamento de Química Física y Química Inorgánica, IU CINQUIMA, Facultad de Ciencias, Universidad de Valladolid, Valladolid 47011, Spain*
[b] *Dipartimento di Chimica G. Ciamician, Università di Bologna, via Selmi 2, Bologna 40126, Italy. E-mail: assimo.maris@unibo.it; Tel: +39 051 2099502*

† Electronic supplementary information (ESI) available: Measured rotational transition lines; experimental rotational spectroscopic parameters of ^{13}C- and OD isotopologues; Kraitchman's substitution coordinates of *cis*-verbenol; theoretical structures of *cis*-verbenol conformers; theoretical structures of *cis*-verbenol···water conformers. See DOI: 10.1039/d0cp00086h

Since the pharmacodynamics and pharmacokinetics processes leading to the drug biological activity are strictly related to the molecular shape and charge distribution,[4] the knowledge of the molecular structure, flexibility and ability to form intra- and inter-molecular non covalent bonds constitutes the first step in understanding and modeling behavior in a biological environment. For this purpose, high resolution rotational spectroscopy combined with quantum mechanical modeling has been extensively exploited to obtain precise and detailed information on organic molecules and their hydrated forms in the isolated phase.

For instance, regarding the monocyclic monoterpenoid *E*-anethole, it has been possible to characterize the structure of two conformers and determine their relative energy.[5] The effects of halogenation on the complex tautomeric equilibrium of 2-hydroxypyridine have been rationalized.[6] The flexibility of antioxidant dihydrolipoic acid has been explored through the investigation of its pharmacophore, 1,3-propanedithiol.[7] The lone pair$\cdots$hole and lone pair$\cdots\pi^*$ interactions have been probed in pentafluoropyridine$\cdots$water[8] and pyridine$\cdots$formaldehyde[9] complexes, respectively. The first steps of solvation have been pointed out comparing the clusters of formamide with 1 to 3 water molecules.[10] Nowadays, owing to the development of the chirped pulse technique,[11] it is possible both to extend the rotational spectroscopic investigation to heavier molecular systems and to obtain quantitative information for analytics purposes, as, for example, in the case of dihydroartemisinic acid, a precursor of anti-malaric artemisin,[12] or for the identification of the gases released during the degradation of methylammonium halide based perovskites.[13] Moreover, new generation spectrometers allow for the discrimination between enantiomers of chiral molecules, as shown in solketal[14] and pulegone[15] studies.

In the present paper, we investigate the microwave broadband spectra of *cis*-verbenol (VRB) and its 1 : 1 complex with water with the aim of determining their structural features and ascertaining which are the dominating non-covalent interactions.

2 Methods

2.1 Experimental details

A broadband spectrum of VRB (4,6,6-trimethyl-bicyclo[3.1.1]hept-3-en-2-ol, $C_{10}H_{16}O$, m.w. 152.23, purity 95%, Sigma Aldrich) was recorded using a chirped-pulse Fourier transform microwave spectrometer (CP-FTMW).[16] A supersonic jet was generated by the expansion of either Ne or Ar at backing pressures of about 2 bar through a 0.8 mm diameter pulse heatable nozzle with pulses of 700–900 μs duration. The sample, placed in the reservoir located at the nozzle, was heated to 363 K and seeded in the expanding gas. The spectrum of the complex of VRB with water was recorded using a mixture of VRB (0.3 g) and water (0.6 g) as the sample and Ne as the carrier gas. The experiment worked at a 5 Hz repetition rate with 5 polarization-detection frames per pulse. Chirp pulses of 4 μs were created by an arbitrary waveform generator and amplified to 20 W. The polarization signal was then radiated from a horn antenna in a direction perpendicular to that of the expanding gas. A molecular transient emission spanning 40 μs is then detected through a second horn, recorded using a digital oscilloscope and Fourier-transformed to the frequency domain. The accuracy of frequency measurements is greater than 10 kHz. Given the low polarization power used, the spectrum was recorded in steps of 2 GHz in the 2–8 GHz frequency range by accumulating a total of 1.6 million spectra per step. The good signal to noise ratio attained allowed us to measure the weak lines belonging to the ^{13}C isotopologues observed in natural abundance.

These spectra were further investigated using a molecular beam Fourier transform spectrometer (MB-FTMW) operating in the 5–13 GHz frequency range.[17] In this experiment, He–Ne mixtures were used at a stagnation pressure of 2 bar expanding in pulses of about 800 μs through a 0.8 mm nozzle. Short (typ. 0.3 μs, 10–300 mW) microwave pulses were used for polarization. Typically, a *ca.* 400 μs-length time domain spectrum was recorded in 40–100 ns intervals and converted to the frequency domain by a fast Fourier transform. Due to the collinear arrangement of the jet and resonator axis, each rotational transition splits into two Doppler components so that the resonant frequencies are taken as the arithmetic mean of both components. Frequency accuracy is better than 3 kHz in this case.

2.2 Computational details

Geometry optimization and harmonic vibrational frequency calculations were run in order to characterize the equilibrium conformers. The MP2/6-311++G(d,p) level of calculation was applied using the Gaussian™‡ computational chemistry software package (G16, Rev. A.03). The hydroxyl internal rotation pathway was explored at the same level of calculation, varying the τ = HO–CH dihedral angle from 0° to 360° with a step of $\Delta\tau = 10°$, whereas all the other parameters were freely optimized.

3 Results and discussion

3.1 Structure of the monomer

Because of the bridged bicyclic structure and the double bond, the skeletal conformation of VRB is locked, and the unique conformational degree of freedom is the internal rotation of the hydroxyl group. Depending on the OH orientation, three staggered conformers are expected (namely *gauche* (G), *anti* (A) and *gauche′* (G′)) depending on the value of the $\tau = \angle$HO–CH dihedral angle (about 60°, 180° and 300°, respectively).

X-ray diffraction studies show that, owing to the formation of two hydrogen bonds, VRB crystallizes in an orthorhombic system with three molecules per asymmetric unit.[18] The conformation of the molecules shown in Fig. 2§ is G′.

‡ Gaussian is a registered trademark of Gaussian, Inc. 340 Quinnipiac St. Bldg. 40 Wallingford, CT 06492 USA.

§ Molecular graphics were obtained with the UCSF Chimera package. Chimera is developed by the Research for Biocomputing, Visualization, and Informatics at the University of California, San Francisco (supported by NIGMS P41-GM103311).

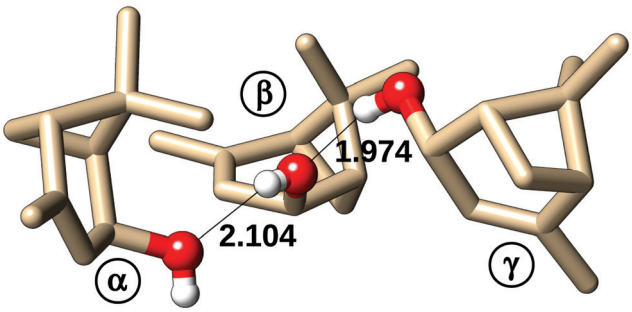

Fig. 2 Asymmetric unit of solid *cis*-verbenol (hydrogen bond distances in Å). Crystal structure from the IUCr electronic archives (Reference: BK1491).

Table 1 MP2/6-311++G(d,p) theoretical rotational constants, quartic centrifugal distortion constants, electric dipole moment components and electronic energy values of VRB conformers

	A	G	G′
A_e/MHz	1312	1319	1327
B_e/MHz	1189	1192	1190
C_e/MHz	911	915	918
D_J/Hz	60.8	63.3	63.9
D_{JK}/Hz	−29.1	−29.3	−31.3
D_K/Hz	0.4	−1.0	1.6
d_1/Hz	−6.3	−7.7	−9.1
d_2/Hz	−2.0	−2.2	−3.6
μ_a/D	0.1	0.6	1.4
μ_b/D	−2.4	0.6	−0.4
μ_c/D	0.3	−1.4	−0.6
E_e/a.u.	−464.607173	−464.606396	−464.606117

The solid-state NMR analyses also demonstrated the presence of a minor metastable polymorph containing a tetramer per asymmetric unit composed of two different conformers. On the basis of *ab initio* calculations, the authors suggest that the involved species are G′ and G, because the A conformation is improbable, due to the sterically unfavorable interactions of the hydroxyl hydrogen atom with the *endo*-methyl (C10) hydrogen atoms.[19]

Based on these considerations, we ran several *ab initio* optimizations at the MP2/6-311++G(d,p) level of calculation. The results relative to the achieved structures are summarized in Table 1 and detailed in the ESI.† In contrast to the behavior in the solid state, in the isolated phase, the A species seems to be the global minimum, with $\Delta E_e(G) = 2.04$ kJ mol^{-1} and $\Delta E_e(G') = 2.77$ kJ mol^{-1}.

To confirm this depiction, the rotational CP-FTMW spectrum was recorded. It appears very dense with a large number of lines, as shown in Fig. 3. Based on the theoretical rotational constants, the most intense of them (34 lines) were easily assigned to μ_b-R-type transitions with the quantum number J ranging from 0 to 5, and a large number of weaker lines (323, with $J = 4$–29) were found to correspond to the μ_b-Q-type transitions. A subsequent search for other kinds of lines allowed us to assign 14 weak μ_c-R-type transitions (with lower J ranging from 0 to 3), whereas no μ_a-type transition lines were observed. No splittings arising from methyl internal rotation were observed in any line. The measured transition lines were fitted to Watson's *S*-reduced semirigid asymmetric rotor Hamiltonian. Since $\kappa = (2B - A - C)/(A - C) = 0.38$ is the asymmetry parameter and VRB is an asymmetric oblate top, the III^l-representation was adopted. The spectroscopic parameters, obtained with the CALPGM suite of programs,[20] are reported in Table 2. The centrifugal distortion constant D_K was found to be non-determinable from the set of lines measured.

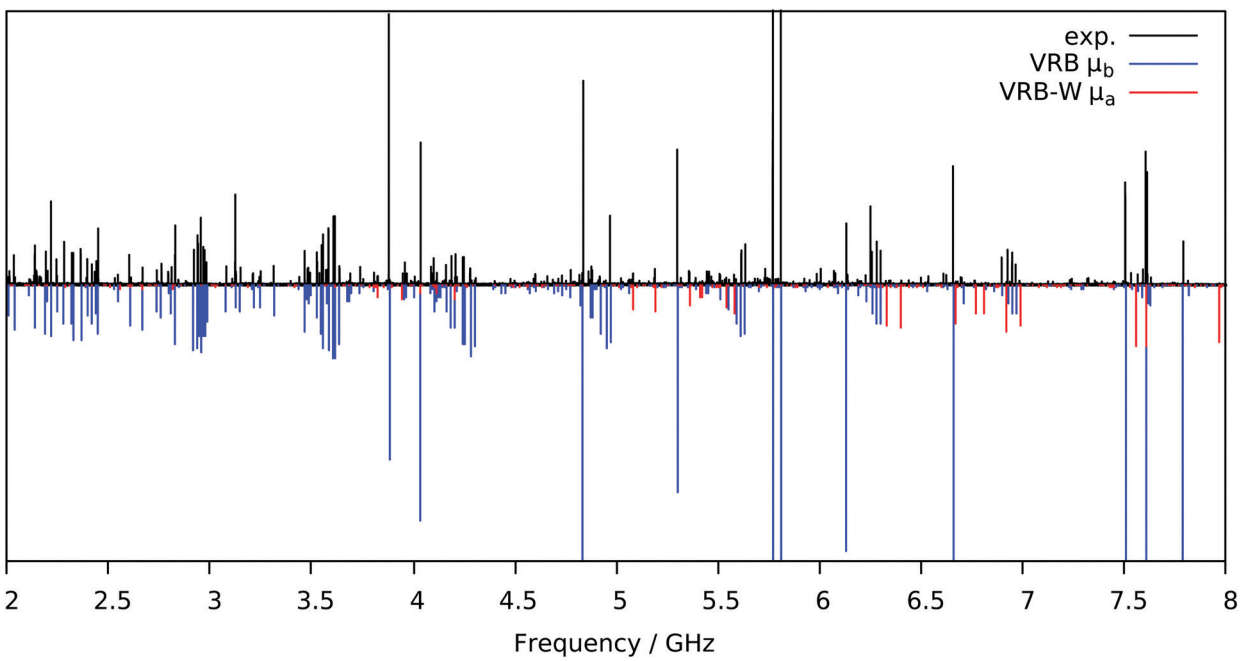

Fig. 3 Comparison between the broadband CP-FTMW rotational spectrum of *cis*-verbenol (upper side, black trace) and the stick simulated spectra of the monomer (μ_b-type, lower side, blue trace) and the water complex (μ_a-type, lower side, red trace) based on the experimentally determined rotational parameters.

Table 2 Experimental rotational constants and quartic centrifugal distortion constants of A-VRB and its 1 : 1 complex with water

	VRB	VRB-W
A_0/MHz	1309.3922(9)[a]	1242.81(2)
B_0/MHz	1185.4415(9)	735.402(1)
C_0/MHz	909.3635(9)	607.988(1)
D_J/kHz	0.07(2)	0.12(2)
D_{JK}/Hz	−29.0(4)	—
d_1/Hz	6.0(1)	—
d_2/Hz	−1.65(6)	—
rms[b]/kHz	7	6
N[c]	371	16

[a] The numbers in parenthesis are the standard errors given in units of the last digit. [b] Root mean square deviation of the fit. [c] Number of lines in the fit.

For a heavy molecule such as VRB, the values of the rotational constants are only slightly affected by the orientation of the hydroxyl hydrogen atom. Thus, additional information is needed to determine which of the three possible conformers the assigned spectrum belongs to. The first indication comes from the components of the electric dipole moment, which are strongly dependent on the hydroxyl orientation. Indeed, a prominent μ_a-, μ_b- or μ_c-type spectrum is predicted for G′, A and G species, respectively, suggesting that the A conformer is the observed one. Moreover, from the relative intensity measurements, a ratio of $\mu_b/\mu_c = 7$ can be estimated, which is in good agreement with the theoretical value ($\mu_b/\mu_c = 8$).

In order to obtain a direct indication of the location of the hydroxyl hydrogen atom, the spectrum of the enriched hydroxyl deuterated isotopologue was also recorded and 13 μ_b-type transition lines with lower $J = 1$–4 were assigned (see the ESI† for the list of transition lines and achieved spectroscopic constants). According to Kraitchman's substitution method,[21] the r_s coordinates of the hydroxyl hydrogen atom were calculated from the rotational constants of the –OH and –OD species (see the ESI†). As shown in Fig. 4, a direct comparison with the equilibrium theoretical structures clearly confirms that the *anti* conformer is observed.

After the assignment of the parent species, some very weak μ_b-type transition lines belonging to the ten ^{13}C-monosubstituted isotopologues were also observed in natural abundance (1.1%).

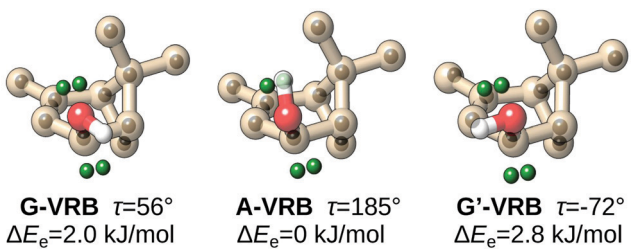

Fig. 4 MP2/6-311++G(d,p) theoretical structures of the *gauche*, *anti* and *gauche′* conformers of *cis*-verbenol with the corresponding relative electronic energy (ΔE_e) and hydroxyl dihedral angle (τ_{HO-CH}). Small spheres represent the experimental substitution structure. Since the sign of r_s coordinates is undetermined, for the hydroxyl H atom, all the plausible combinations are shown. A comparison between structures unequivocally shows that the *anti* conformer is observed.

Exploiting the sensitivity of the MB-FTMW spectrometer, 10 lines with lower $J = 1$–3 were assigned for each isotopologue, allowing us to determine the corresponding rotational constants (while the centrifugal distortion constants were fixed to zero) and the r_s coordinates represented in Fig. 4 (all data are given in the ESI†). As can be seen in this figure and in Table S13 of the ESI,† the substitution coordinates match very well to the calculated equilibrium structure, supporting the identification of A-VRB as the observed conformer.

3.2 Potential energy for hydroxyl rotation

It is worth noting that in spite of the steric hindrance of the *endo* methyl group (C10), in the gas phase, the most stable conformation of VRB is the same as that of smaller linear analogues such as allyl alcohol[22,23] and 3-buten-2-ol,[24] which share with VRB the same C=C–C–OH fragment. For these molecules, since the hydroxyl H atom is oriented toward the π-bond, an attractive intramolecular interaction has been suggested.[25] In order to point out the effect of the substituting groups, the hydroxyl internal rotational pathways of allyl alcohol, (*R*)-3-buten-2-ol, (+)-*cis*-verbenol and (+)-*trans*-verbenol were computed at the MP2/6-311++G(d,p) level. The achieved potential energy surfaces are compared in Fig. 5.

In agreement with experimental data, the A species are the most stable for all molecules. The energy gap between A and the G and G′ species decreases when the steric hindrance increases and VRB's conformational interconversion pathway is the flattest one. Low conformational barriers can be easily overcome during supersonic expansion.[26] Under pre-expansion conditions, the estimated relative population ratio is G : A : G′ = 0.5 : 1 : 0.4, but no transition lines of G and G′ were observed, using Ar or Ne as the carrier gases, indicating that a strong relaxation process toward the global minimum took place in the supersonic expansion.

3.3 Structure of the complex

Concerning the 1 : 1 complex of VRB with water (VRB-W), both units can act both as a proton donor and a proton acceptor. The rotational spectroscopy studies on methanol,[27] ethanol,[28] isopropanol,[29] *tert*-butanol,[30] *n*-propanol-water,[31] and cyclohexanol[32] have shown that water serves as a proton donor with respect to alkyl alcohols. Otherwise, water acts as proton acceptor in the case of phenol[33] and perfluorinated compounds (hexafluoroisopropanol).[34]

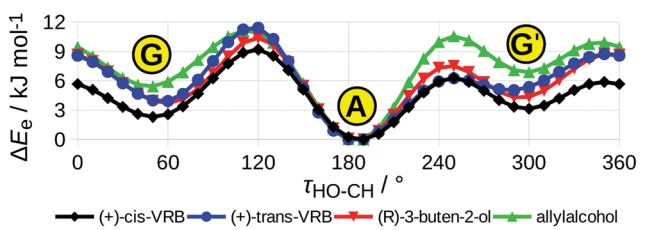

Fig. 5 MP2/6-311++G(d,p) theoretical hydroxyl rotation pathways of allyl-alcohol analogues: (+)-*cis*-verbenol, (+)-*trans*-verbenol, (*R*)-3-buten-2-ol, and allyl alcohol.

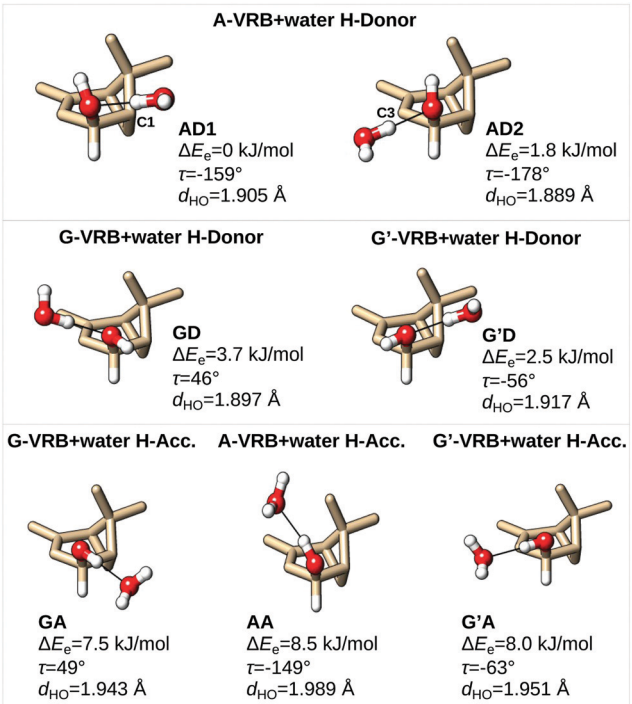

Fig. 6 MP2/6-311++G(d,p) theoretical structures, relative electronic energy (ΔE_e), hydroxyl dihedral angle (τ_{HO-CH}) and intermolecular hydrogen bond length (d_{HO}) of the VRB-W complexes.

Theoretical analysis of VRB-W results in the seven structures listed in the ESI† and shown in Fig. 6 with relative electronic energy values, hydrogen bond distances and hydroxyl dihedral angles (τ_{HO-CH}). The complexes are labeled with a two-letter code indicating the conformation of VRB (G/A/G′) and the donor (D) or acceptor (A) role of water with respect to the hydroxyl group of VRB.

The stability decreases as AD1 > AD2 > G′D > GD > GA > G′A > AA. As observed for the aforementioned alkyl alcohols, the most stable geometries involve a proton donor water molecule. Interestingly, VRB's A arrangement is strongly destabilized when water acts as the proton acceptor. Two plausible reasons can be hypothesized. The first one is that insertion of water prevents the formation of the OH···π intramolecular interaction responsible for the stability of the A conformation. The second one is that, upon hydrogen bond formation, verbenol's hydroxyl group is predicted to rotate by about 26° with respect to the isolated structure. This rearrangement in the large monomer, probably due to the steric hindrance of the *endo*-methyl group (C10), could reasonably affect the overall stability of the AA species. Anyway, the conformational behavior of VRB is predicted to be sensitive to the interaction with water. A similar effect has been experimentally evidenced in the cases of flexible 12-crown-4 ether,[35] 15-crown-5-ether,[36] and aminoethanol,[37] for which structural changes can be induced by hydrogen bond formation.

With regard to the AD species, the hydrogen atom of water can bind with the two different lone pairs of oxygen, giving rise to two different species: AD1 and AD2. Although AD1 is predicted to be the most stable, the hydrogen bond distance in AD2 is shorter by 0.016 Å. However, the $H_2O\cdots HC1$ distance in AD1 (2.567 Å) is shorter than the $H_2O\cdots HC3$ distance in AD2 (2.742 Å), suggesting that the secondary interaction between the oxygen atom of water and the hydrogen atoms of VRB plays a significant role in determining the conformational preferences.

Table 3 MP2/6-311++G(d,p) theoretical electronic energy values (a.u.), rotational constants (MHz) and electric dipole moment component (D) of VRB-W conformers

	E_e	A_e	B_e	C_e	μ_a	μ_b	μ_c
AD1	−540.894589	1248	728	600	2.1	−0.4	−0.8
AD2	−540.893903	1210	674	555	2.8	0.6	0.1
AA	−540.891332	1045	752	652	−1.2	−0.2	−2.2
GD	−540.893163	1144	708	597	−3.5	−0.8	0.3
GA	−540.891724	1205	656	544	3.0	−0.8	0.9
G′D	−540.893636	1265	753	625	−1.6	2.2	−0.1
G′A	−540.891544	1198	656	544	−3.0	1.0	0.2

The same kind of considerations can be extended to the G′D/GD pair. Indeed, with regard to the monomers, G is more stable than G′ by 0.7 kJ mol^{-1}, whereas the G′D complex is more stable than GD by 1.2 kJ mol^{-1}. Again, the less stable complex exhibits a shorter hydrogen bond distance (by 0.020 Å) and a larger secondary interaction distance: 2.913 against 2.641 Å.

In order to benchmark these quantum mechanical results, experimental spectra of the water adduct were collected. Several new μ_a-R-type transition lines, with lower J = 2–5, were observed and fitted to the Watson's semirigid asymmetric rotor Hamiltonian. Since VRB-W is an asymmetric prolate top (κ = −0.60), the I^r-representation was adopted. The achieved rotational constants and D_J centrifugal distortion constants are reported in Table 2. A comparison with the predicted spectroscopic parameters for VRB-W (Table 3) indicates that the spectrum belongs to the AD1 species, in agreement with the theoretical predictions.

As final remarks, we consider the crystal structure of VRB,[18] whose asymmetric unit consists of three VRB moieties connected through a hydrogen bond chain among hydroxyl groups: O–H···O–H···O–H. The side units act as a proton acceptor (α in Fig. 2) and a proton donor (γ in Fig. 2) whereas the central unit (β in Fig. 2) plays a double role. Notice that to behave as a proton donor, due to steric hindrance, the moieties cannot be in the *anti* conformation, indeed all of them are *gauche*′. This seems to be in agreement with our calculations, showing that the stabilization of the G′ form, rather than the G form, can take place upon hydrogen bond formation.

4 Conclusions

Based on the rationalization of the parameters determined from the analysis of the microwave broadband spectra, we determined the experimental molecular structure of VRB and its weakly bound 1:1 complex with water. In both cases, a unique dominant conformation was observed, with no evidence of higher-energy conformers. Under isolated conditions, the *anti* conformation, with the hydrogen atom pointing towards the ring system, is preferred to the *gauche* and *gauche*′ ones where one of the lone pairs of the oxygen atom faces the ring system.

The formation of the hydrogen bond with the water molecule acting as the proton donor does not alter this arrangement, which is typical of allyl alcohol compounds. In contrast, the *ab initio* calculations show that when VRB acts as the proton donor, the *anti* species become less stable, suggesting the dependence of the conformational preferences of this terpenoid on the surrounding interactions. The environment in which VRB is located can act as a switch, indicating its role as a proton acceptor or proton donor, thus enabling it to completely change the chemical reactivity of VRB and directing the implied biological processes along completely different pathways.

Conflicts of interest

There are no conflicts to declare.

Acknowledgements

This work has been supported by the Ministerio de Economía y Competitividad (Grant CTQ2016-75253-P) and the University of Bologna.

Notes and references

1 J. Gershenzon and N. Dudareva, *Nat. Chem. Biol.*, 2007, **3**, 408–414.
2 J. Brand, J. Bracke, A. Markovetz, D. Wood and L. Browne, *Nature*, 1975, **254**, 136–137.
3 C. Chiua, C. Keelinga and J. Bohlmanna, *Nature*, 2018, **115**, 3652–3657.
4 D. Stepensky, *Clin. Pharmacokinet.*, 2013, **52**, 415–431.
5 C. Calabrese, Q. Gou, A. Maris, S. Melandri and W. Caminati, *J. Phys. Chem. B*, 2016, **120**, 6587–6591.
6 C. Calabrese, A. Maris, I. Uriarte, E. Cocinero and S. Melandri, *Chem. – Eur. J.*, 2017, **23**, 3595–3604.
7 A. Vigorito, C. Calabrese, E. Paltanin, S. Melandri and A. Maris, *Phys. Chem. Chem. Phys.*, 2017, **19**, 496–502.
8 C. Calabrese, Q. Gou, A. Maris, W. Caminati and S. Melandri, *J. Phys. Chem. Lett.*, 2016, **7**, 1513–1517.
9 S. Blanco and J. López, *J. Phys. Chem. Lett.*, 2018, **9**, 4632–4637.
10 S. Blanco, P. Pinacho and J. López, *J. Phys. Chem. Lett.*, 2017, **8**, 6060–6066.
11 G. B. Park and R. Field, *J. Phys. Chem.*, 2016, **144**, 20090.
12 J. Neill, Y. Yang, M. Muckle, R. Reynolds, L. Evangelisti, R. Sonstrom, B. Pate and B. Gupton, *Org. Process Res. Dev.*, 2019, **23**, 1046–1051.
13 E. Juarez-Perez, L. Ono, I. Uriarte, E. J. Cocinero and Y. Qi, *ACS Appl. Mater. Interfaces*, 2019, **11**, 12586–12593.
14 S. Lobsiger, C. Pérez, L. Evangelisti, K. Lehmann and B. Pate, *J. Phys. Chem.*, 2015, **6**, 196–200.
15 A. Krin, C. Pérez, P. Pinacho, M. Quesada-Moreno, J. López-González, J. R. Avilés-Moreno, S. Blanco, J. C. López and M. Schnell, *Chem. – Eur. J.*, 2018, **24**, 721–729.
16 G. Brown, B. Dian, K. Douglass, S. Geyer, S. Shipman and B. Pate, *Rev. Sci. Instrum.*, 2008, **79**, 4–5.
17 J. Alonso, F. Lorenzo, J. López, A. Lesarri, S. Mata and H. Dreizler, *Chem. Phys.*, 1997, **218**, 267–275.
18 J. Harper, A. Arif and D. Grant, *Acta Crystallogr., Sect. C: Cryst. Struct. Commun.*, 2000, **56**, 451–452.
19 J. Harper and D. Grant, *J. Am. Chem. Soc.*, 2000, **122**, 3708–3714.
20 H. Pickett, *J. Mol. Spectrosc.*, 1991, **148**, 371–377.
21 J. Kraitchman, *Am. J. Phys.*, 1953, **21**, 17–25.
22 H. Badawi, P. Lorencak, K. W. Hillig II, M. Imachi and R. Kuczkowski, *J. Mol. Struct.*, 1987, **162**, 247–254.
23 S. Melandri, P. Favero and W. Caminati, *Chem. Phys. Lett.*, 1984, **223**, 541–545.
24 Z. Smith, N. Carballo, E. Wilson, K. Marstokk and H. Moellendal, *J. Am. Chem. Soc.*, 1985, **107**, 1951–1957.
25 B. Miller, J. Lane and H. Kjaergaard, *Phys. Chem. Chem. Phys.*, 2011, **13**, 14183–14193.
26 R. S. Ruoff, T. D. Klots, T. Emilson and H. S. Gutowski, *J. Chem. Phys.*, 1990, **93**, 3142–3150.
27 P. Stockman, G. Blake, F. Lovas and R. Suenram, *J. Chem. Phys.*, 1997, **107**, 3782–3790.
28 I. Finneran, P. Carroll, M. Allodi and G. Blake, *Phys. Chem. Chem. Phys.*, 2015, **17**, 24210–24214.
29 L. Evangelisti, Q. Gou, G. Feng, W. Caminati, G. J. Mead, I. A. Finneran, P. B. Carroll and G. A. Blake, *Phys. Chem. Chem. Phys.*, 2017, **19**, 568–573.
30 L. Evangelisti and W. Caminati, *Phys. Chem. Chem. Phys.*, 2010, **12**, 14433–14441.
31 G. Mead, E. Alonso, I. Finneran, P. Carroll and G. Blake, *J. Mol. Spectrosc.*, 2017, **335**, 66–73.
32 M. Juanes, W. Li, L. Spada, L. Evangelisti, A. Lesarri and W. Caminati, *Phys. Chem. Chem. Phys.*, 2019, **21**, 3676–3682.
33 S. Melandri, A. Maris, P. Favero and W. Caminati, *Chem. Phys.*, 2002, **283**, 185–192.
34 A. Shahi and E. Arunan, *Phys. Chem. Chem. Phys.*, 2015, **17**, 24774–24782.
35 C. Pérez, J. López, S. Blanco and M. Schnell, *J. Phys. Chem. Lett.*, 2016, **7**, 4053–4058.
36 J. López, C. Pérez, S. Blanco, V. Shubert, B. Themelso, G. Shields and M. Schnell, *Phys. Chem. Chem. Phys.*, 2019, **21**, 2875–2881.
37 S. Melandri, A. Maris and L. Favero, *Mol. Phys.*, 2010, **108**, 2219–2223.